THE JOURNAL OF PHYSICAL CHEMISTRY B

Article

Cite This: J. Phys. Chem. B 2018, 122, 4035−4044

pubs.acs.org/JPCB

Cyanamide as an Infrared Reporter: Comparison of Vibrational Properties between Nitriles Bonded to N and C Atoms

Giseong Lee,[‡,∥] Dorota Kossowska,[†,‡,∥] Joonhyung Lim,[†,‡] Soobin Kim,[†] Hogyu Han,*[,‡] Kyungwon Kwak,*[,†,‡] and Minhaeng Cho*[,†,‡]

[†]Center for Molecular Spectroscopy and Dynamics, Institute for Basic Science (IBS), Seoul 02841, Korea

[‡]Department of Chemistry, Korea University, Seoul 02841, Korea

Supporting Information

ABSTRACT: Infrared (IR) probes based on terminally blocked β-cyanamidoalanine (AlaNHCN) **1** and p-cyanamidophenylalanine (PheNHCN) **2** were synthesized, and the vibrational properties of their CN stretch modes were studied using Fourier transform infrared (FTIR) and femtosecond IR pump−probe spectroscopies in combination with quantum chemical calculations. From FTIR studies, it is found that the transition dipole strengths of the cyanamide (NHCN) group in **1** and **2** are much larger than those of the nitrile (CN) group but comparable to those of the isonitrile (NC) and azido (N_3) groups in their previously studied analogs. The CN stretch frequencies in **1** and **2** are red-shifted from those in their nitrile analogs but more blue-shifted from the NC and N_3 stretch frequencies in their isonitrile and azido analogs. The much larger transition dipole strength and the red-shifted frequency of the cyanamide relative to nitrile group originates from the n → π^* interaction between the N atom's nonbonding (n) and CN group's antibonding (π^*) orbitals of the NHCN group. Unlike aliphatic cyanamide **1**, aromatic cyanamide **2** shows a complicated line shape of the CN stretch spectra. Such a complicated line shape arises from the Fermi resonance between the CN stretch mode of the NHCN group and one of the overtones of the phenyl ring vibrations and can be substantially simplified by deuteration of the NHCN into NDCN group. From IR pump−probe experiments, the vibrational lifetimes of the CN stretch mode in **1** were determined to be 0.58 ± 0.04 ps in D_2O and 0.89 ± 0.09 ps in H_2O and those in **2** were determined to be 1.64 ± 0.13 ps in CH_3OD/dimethyl sulfoxide and 0.30 ± 0.05 and 2.62 ± 0.26 ps in CH_3OH. The short time component (0.30 ± 0.05 ps) observed for **2** in CH_3OH is attributed to the vibrational relaxation through Fermi resonance. These vibrational lifetimes are close to those of the nitrile and azido groups but shorter than those of the isonitrile group. Consequently, cyanamide behaves like an apparent vibrational hybrid of nitrile and isonitrile in that cyanamide is similar to nitrile in vibrational frequency and lifetime but to isonitrile in transition dipole strength. It is believed that cyanamide has the potential to be a strongly absorbing IR reporter of the conformational and environmental structure and dynamics of biomolecules in comparison to nitrile, a weak absorber.

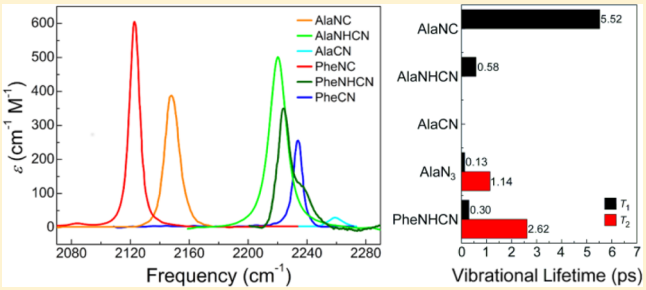

Downloaded via UNIV OF CAMBRIDGE on January 22, 2021 at 14:13:00 (UTC).
See https://pubs.acs.org/sharingguidelines for options on how to legitimately share published articles.

I. INTRODUCTION

Ultrafast infrared (IR) spectroscopy is a powerful tool for assessing the structural and environmental dynamics of biomolecules.[1−6] Numerous IR probes based on biomolecules have been used to site-specifically interrogate their structure and dynamics.[7−12] Although many IR probes are found to be useful in Fourier transform infrared (FTIR) spectroscopy, their use in the time-resolved nonlinear IR spectroscopy is often limited by the lack of some desired spectral properties. Such properties include large transition dipole moment, narrow bandwidth, long vibrational lifetime, and high environmental sensitivity. Moreover, the small size and high solvothermal stability of an IR reporter incorporated into biomolecules are required.

The stretch vibration of the nitrile (C≡N) group is a useful IR reporter of the structure and dynamics of local environment.[13−29] In particular, the nitrile stretch frequency is sensitively blue-shifted upon hydrogen bonding (H-bonding), which is mainly due to the exchange-repulsion solute−solvent interaction.[12] However, the nitrile stretch mode exhibits a small transition dipole strength (<1.0 × 10^{-2} D^2)[30,31] and a substantial overlap with a broad O−D stretch band of D_2O, whereby it is sometimes hard to obtain high-quality nonlinear IR signals. Compared to aromatic nitriles, aliphatic ones have about 10 times smaller transition dipole strength and thus are far less commonly used IR probes in nonlinear IR spectroscopy. The vibrational lifetime of the CN group is very short (<5.0 ps) but can be extended somewhat by isotopic substitution.[25]

The CN stretch modes of the thiocyanato (S−C≡N) and selenocyanato (Se−C≡N) groups receive particular attention because their vibrational lifetimes are much longer than those of any other vibrational modes studied so far.[32−44] It is found

Received: January 25, 2018
Revised: March 7, 2018
Published: March 8, 2018

© 2018 American Chemical Society

DOI: 10.1021/acs.jpcb.8b00887
J. Phys. Chem. B 2018, 122, 4035−4044

that Se atom is more effective than S atom in extending the vibrational lifetime of the CN stretch mode. The vibrational lifetime of the SCN group is several tens of ps, whereas that of the SeCN group exceeds 100 ps.[41] However, the small transition dipole strength of these groups, which is comparable to that of the CN group bonded to C atom, limits their use for the nonlinear IR study of protein dynamics, even when the site-specific introduction of these groups into proteins can be easily achieved by converting cysteine thiols into them.[32]

The asymmetric stretch vibration of the azido (N_3) group is another type of the widely used IR reporter of protein structure and dynamics.[45−59] This is mainly due to its large transition dipole strength (>4.5 × 10^{-2} D^2),[30,31] which makes it feasible to carry out the nonlinear IR study of proteins at low concentrations. Nevertheless, azido probes have some drawbacks such as a broad bandwidth and a short vibrational lifetime (<1.5 ps). It is often the case that the azido stretch band overlaps with the accidental Fermi resonance band, which impedes the quantitative analysis of the resulting complicated spectrum.[55,57−59] The accidental Fermi resonance has been also observed for other IR reporters[13,14,60,61] and can often be modulated by isotopic substitution.[58]

The amide I mode of the peptide group is one of the most effective IR reporters of protein secondary structures.[62−64] Its secondary structure sensitivity results from coupling among amide I oscillators that leads to vibrational states delocalized over large regions of the protein. However, such delocalized vibrations obscure the local structural information included in the native amide I band, which can be recovered by site-specific introduction of structurally nonperturbative $^{13}C^{18}O$ labels into the protein backbone. The C≡O stretch vibration of metal carbonyls attracts much interest because of their significantly higher extinction coefficients than those of any other IR reporters of proteins in the transparent IR window of aqueous protein solutions.[65−67] However, one possible drawback of these metal carbonyls is that they are comparatively large and thus structurally more perturbative.

Recently, we reported the IR study of the isonitrile (N≡C) group in comparison with the nitrile and azido groups.[30,31] In H-bonding solvents, the vibrational frequency shifts of isonitriles are larger than those of nitriles. In addition, the transition dipole strength of the isonitrile group (>2.2 × 10^{-2} D^2)[30,31] is much larger than that of the nitrile group and almost comparable to that of the azido group. Moreover, its vibrational lifetime (>5.0 ps) is longer than that of the nitrile and azido groups. Accordingly, isonitrile can be a better IR reporter of H-bonding structure and dynamics than nitrile and azide despite its less chemical stability under acidic conditions.

Here, we report novel IR probes based on terminally blocked cyanamide (NHCN)-derivatized alanine **1** (Ac-Ala(NHCN)-NHMe, Figure 1) and phenylalanine **2** (Ac-Phe(NHCN)-NHMe) containing cyanamide (HN−C≡N), a seemingly hybrid form of mainly C≡N and partially N≡C. It is noteworthy that there is a structural similarity between cyanamide (HN−C≡N) and azide (HN−N≡N ↔ HN═N═N). The vibrational properties of the CN stretch mode in **1** and **2** were investigated using FTIR and femtosecond IR pump−probe spectroscopies. It is found that the transition dipole strength of cyanamide is much larger than that of nitrile but comparable to that of isonitrile and azide. The vibrational frequency of cyanamide is red-shifted from that of nitrile but more blue-shifted from that of isonitrile and azide. The vibrational lifetime of cyanamide is close to that of nitrile and azide but shorter than that of isonitrile. Consequently, cyanamide is similar to nitrile in vibrational frequency and lifetime, to isonitrile in transition dipole strength, and to azide in transition dipole strength and vibrational lifetime. Thus, cyanamide is believed to be a strongly absorbing IR reporter in comparison to nitrile, a weak absorber. To explain the differences in vibrational properties between cyanamide and nitrile, quantum chemical calculations were performed. We found that such differences are associated with the occurrence of the n → π^* interaction between the N atom's nonbonding (n) and CN group's antibonding (π^*) orbitals in cyanamide but not in nitrile. Quantum chemical calculations also reveal that a complicated line shape of the CN stretch spectra in aromatic cyanamide is attributed to the Fermi resonance, which does not occur in aromatic nitrile.

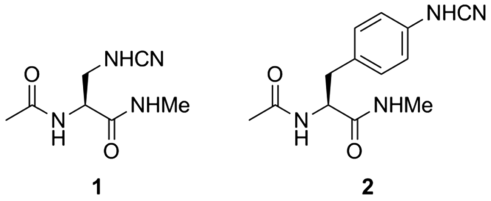

Figure 1. Structures of IR probes **1** and **2**.

II. EXPERIMENTAL AND COMPUTATIONAL METHODS

II.I. Materials. Compounds **1** and **2** were synthesized and characterized (Scheme 1 and Section SII in the Supporting Information). All of the solvents for IR spectroscopy were purchased from Sigma-Aldrich and used as received. To prepare deuterated samples, the samples were dissolved in D_2O, dried, and then dissolved in deuterated solvents for FTIR studies, whereas they were directly dissolved in deuterated solvents for IR pump−probe experiments. The deuteration of the NHCN into NDCN group was monitored by the disappearance of ^1H NMR peaks around 6.81 and 10.05 ppm for **1** and **2** in DMSO-d_6, respectively. To examine the solvothermal stability of the NHCN group, we performed TLC analyses for **1** and **2** subjected to various concentrations of methanolic HCl and

Scheme 1. Syntheses of 1 and 2[a]

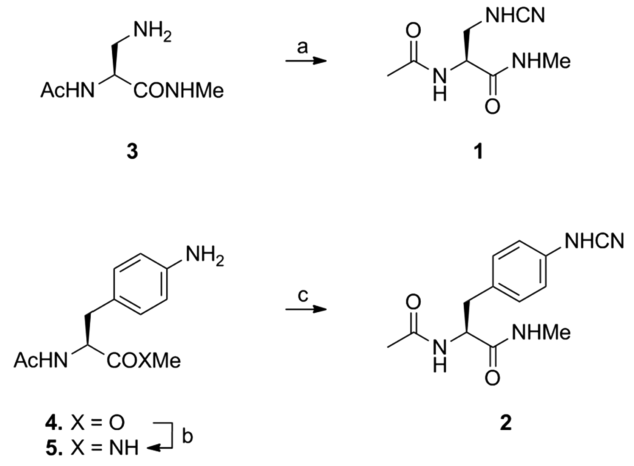

[a]Reagents and conditions: (a) BrCN, Me_3N, tetrahydrofuran (THF), 0 °C, 72%; (b) 40% $MeNH_2$, MeOH, rt, 100%; (c) BrCN, THF/Et_2O (1:1), 65 °C, 56%.

DOI: 10.1021/acs.jpcb.8b00887
J. Phys. Chem. B 2018, 122, 4035−4044

methylamine solutions at varying temperatures with stirring. It is found that the chemical stabilities (<1% decomposition) of the NHCN group in **1** and **2** at room temperature are maintained at pH 0−2 for <10 min and at pH 3−6 for >24 h, and at a methylamine concentration of 0.1 M for <10 min and >24 h, respectively. In addition, the thermal stabilities of the NHCN group in **1** and **2** at a neutral pH are found to be maintained at <35 and 80 °C for >24 h, respectively. Thus, the NHCN groups in both **1** and **2** are unstable under acidic conditions (<pH 2) and these groups in **1** are thermally less stable than those in **2**.

II.II. FTIR and Polarization-Controlled IR Pump−Probe Spectroscopies. For FTIR and IR pump−probe experiments, the samples were placed in a home-made IR cell confined with two CaF_2 windows (3 mm thickness each) and a Teflon spacer (12 μm thickness for aqueous samples and 25 μm for other samples) at various concentrations to give an absorbance of ~0.3.

FTIR spectra were measured on a Bruker VERTEX 70 spectrometer with a frequency resolution of 1 cm^{-1} at 22 °C.

The femtosecond laser setup and experimental details for polarization-controlled IR pump−probe spectroscopy have been described elsewhere.[68] Briefly, a femtosecond Ti:sapphire oscillator (Tsunami, Spectra-Physics) and a regenerative amplifier (Spitfire, Spectra-Physics) are used to generate 800 nm pulse, which then pumps an optical parametric amplifier (OPA-800C, Spectra-Physics) to produce near-IR pulses centered at ~1.4 μm (signal) and ~1.9 μm (idler). The near-IR pulse is then focused onto a 2.0 mm thick $AgGaS_2$ crystal, where mid-IR pulse centered at ~2230 cm^{-1} with a bandwidth (full width at half-maximum (FWHM)) of ~150 cm^{-1} and a repetition rate of 1 kHz is produced through a difference frequency generation process. Subsequently, the mid-IR pulse is split using a ZnSe beam splitter into pump and time-delayed probe pulses with an intensity ratio of 9:1. The time delay between the two pulses is controlled using a motorized linear stage placed in the probe beam line. Afterward, both pulses are focused onto a sample and the generated pump−probe signal is frequency-resolved with a monochromator and detected at each time delay using a 32-element mercury cadmium telluride (MCT) array detector. The average power of the pump pulse, measured in front of the sample, was ~45.0 μW. As a consequence of both vibrational and rotational relaxation processes, the intensity of the signal decays as the time delay increases. The pump−probe signal is measured with two different polarizations of the probe beam, that is, parallel ($S_{\parallel}(t)$) and perpendicular ($S_{\perp}(t)$) to the polarization direction of the pump beam, to separate the vibrational and rotational contributions to the overall decay signal. From these two signals, the isotropic ($S_{iso}(t)$) signal associated with vibrational population ($P(t)$) decay can be obtained using the following relation

$$S_{iso}(t) = S_{\parallel}(t) + 2S_{\perp}(t) = 3P(t) \quad (1)$$

II.III. Quantum Chemical Calculations. The ab initio calculations of the four model systems, CH_3X and C_6H_5X in H_2O (X = NHCN) and D_2O (X = NDCN) with the Onsager continuum solvation model, were performed by Kohn-Sham formulation of density functional theory (KS-DFT). B3LYP (Becke, three-parameter, Lee−Yang−Parr)[69,70] exchange−correlation functional was employed for all of the calculations. Geometry optimizations and subsequent harmonic and anharmonic frequency calculations were performed using a 6-311++G** basis set. All of the calculations were carried out using Gaussian 09 suite of packages.[71]

III. RESULTS AND DISCUSSION

III.I. FTIR Spectroscopy. To obtain the information about the solvatochromic behavior of cyanamide probes, the FTIR spectra of **1** and **2** in the CN stretch region were investigated with various solvents (Figure 2). The detailed analysis of each spectrum is given in Tables 1 and S1−S3 in the Supporting

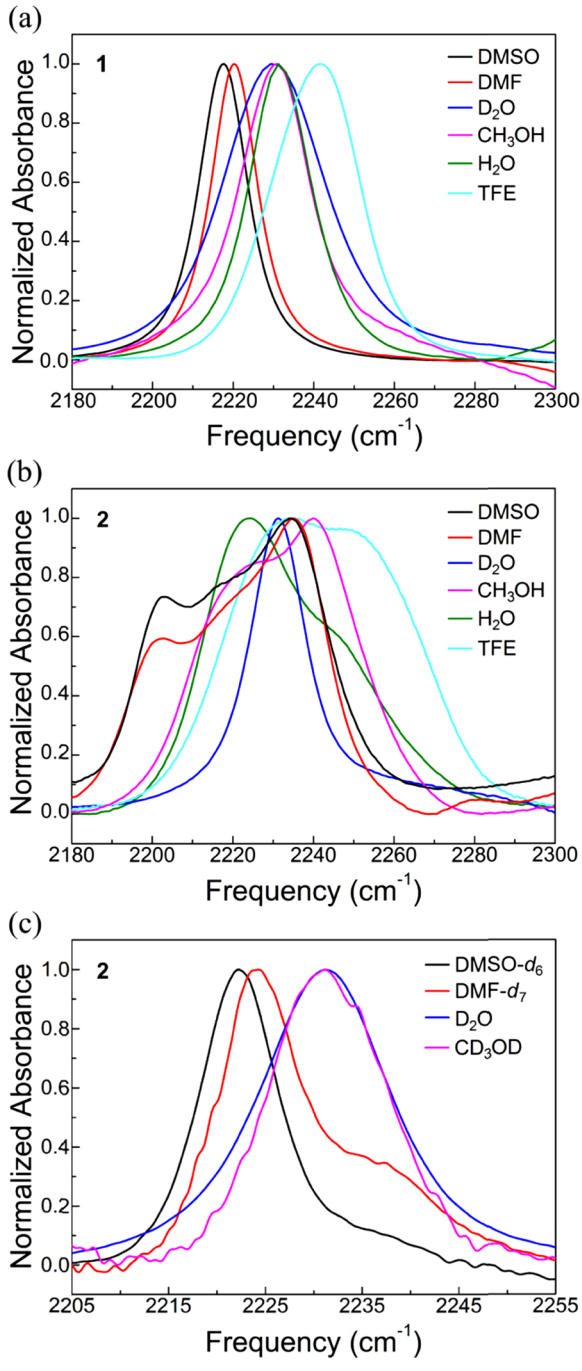

Figure 2. Solvent-dependent FTIR spectra of **1** and **2**. In (c), the samples were deuterated with D_2O and then dried before they were dissolved in deuterated solvents. TFE stands for 2,2,2-trifluoroethanol. For spectral analyses, see Figures S1−S4 and Tables S1−S3 in the Supporting Information.

DOI: 10.1021/acs.jpcb.8b00887
J. Phys. Chem. B 2018, 122, 4035−4044

Table 1. Spectral Properties of 1 and 2 in Various Solvents[a]

	1				2								
	D_2O	H_2O	CH_3OH	DMF	D_2O	H_2O		CH_3OH		CH_3OD/DMSO	DMF-d_7		
ω_0 (cm^{-1})	2230.2	2231.7	2230.3	2220.3	2231.4	2223.1	2247.5	2220.4	2243.1	2225.2	2224.3	2236.1	
FWHM (cm^{-1})	30.1	18.8	21.5	14.0	16.5	24.1	28.2	26.2	23.9	11.8	9.4	15.5	
ε (cm^{-1} M^{-1})[b]	377	406	358	501	610	413		344		655	350		
D (10^{-2} D^2)[c]	6.25	3.76	3.44	3.78	3.28	7.41		6.72		4.47	2.33		
T_1 (ps)[d]	0.58 ± 0.04	0.89 ± 0.09						0.30 ± 0.05 (0.78)		1.64 ± 0.13			
								2.62 ± 0.26 (0.22)					

[a]Fitting parameters obtained from the Voigt fitting analyses of the FTIR spectra in Figure 2 (ω_0, FWHM, ε, and D; see Figures S1 and S2 in the Supporting Information) and the multiexponential fitting analyses of the IR pump−probe signal decays in Figure 4 (T_1). [b]The ε values for **2** in H_2O, CH_3OH, and DMF-d_7 were measured around 2223.1, 2243.1, and 2224.3 cm^{-1}, respectively (see Figures S3 and S4 in the Supporting Information). [c]Ref 77. [d]Relative amplitudes in parentheses.

Information. The FTIR spectra of studied compounds significantly differ between polar protic (water, methanol, and 2,2,2-trifluoroethanol (TFE)) and aprotic (dimethylformamide (DMF) and dimethyl sulfoxide (DMSO)) solvents. In the case of **1**, we can see a strong frequency blue shift of the CN stretch band, a singlet, in protic solvents relative to aprotic ones. Such a frequency blue shift was also observed for **2**. Intriguingly, however, a noticeable difference in the spectral line shape of the CN stretch band between protic and aprotic solvents was additionally observed for **2**. In aprotic solvents, we can see a complicated line shape, which can be fitted to three Voigt functions, whereas in protic solvents, the spectra are doublets (NHCN) or singlets (NDCN formed upon deuteration of NHCN). More detailed line shape analyses of the FTIR spectra in all solvents will be described later.

The most interesting feature of our new probes, however, is the large transition dipole strength of their cyanamide group. The transition dipole strengths (in units of 10^{-2} D^2) of the cyanamide group in **1** are 6.25 in D_2O and 3.78 in DMF and those in **2** are 3.28 in D_2O and 2.33 in DMF-d_7 (Table 1). Note that the transition dipole strengths of the nitrile, isonitrile, and azido groups in their alanine analogs are 0.06, 1.82, and 5.49 in D_2O and 0.15, 2.21, and 4.80 in DMF and those in their phenylalanine analogs are 0.99, 2.71, and 12.9 in DMF, respectively.[30,31] Thus, the transition dipole strengths of the cyanamide group in **1** and **2** are much larger than those of the nitrile group but comparable to those of the isonitrile and azido groups in their analogs. In addition, the transition dipole strengths of aliphatic cyanamide **1** are comparable to those of aromatic cyanamide **2**, whereas the much smaller (comparable) transition dipole strengths were observed for their aliphatic nitrile (isonitrile and azido) analogs in comparison to aromatic ones. The large transition dipole strength of the cyanamide group allows our new probes to be used for the nonlinear IR study of proteins at relatively low concentrations.

The CN stretch spectra of **1** in both polar protic and aprotic solvents are a singlet at center frequencies of 2217.5−2240.5 cm^{-1} with bandwidths (FWHM) of 14.0−30.1 cm^{-1} (see Figure 2a and Table S1 in the Supporting Information). The spectra of **1** in D_2O, H_2O, CH_3OH, and TFE are centered at 2230.2, 2231.7, 2230.3, and 2240.5 cm^{-1} with bandwidths of 30.1, 18.8, 21.5, and 26.0 cm^{-1}, respectively. Thus, the frequency blue shift (CH_3OH < H_2O < TFE) and bandwidth broadening (H_2O < CH_3OH < TFE) are more pronounced in proportion to the H-bond donating ability of the protic solvents (CH_3OH < H_2O < TFE; Kamlet−Taft parameters α of 0.93, 1.17, and 1.51 for CH_3OH, H_2O, and TFE, respectively).[72] Note that the frequency blue shift and bandwidth broadening were the largest for TFE, the strongest H-bond donor among the solvents considered here.[73,74] The frequency blue shift in D_2O is similar to that in H_2O, whereas the bandwidth broadening in D_2O is more substantial than that in H_2O. Thus, the deuteration of the NHCN into NDCN group results in the significant bandwidth broadening without the large frequency red shift. A notable increase in transition dipole strength from 3.76 to 6.25 without a concomitant increase in extinction coefficient upon deuteration of the NHCN into NDCN group is observed, which is due to the significant bandwidth broadening without the large increase in absorbance at the center frequency. The spectrum of **1** in CH_3OH is similar to that in H_2O with a little less blue-shifted center frequency and a little bit broader bandwidth. The spectra of **1** in DMF and DMSO are centered at 2220.3 and 2217.5 cm^{-1} with bandwidths of 14.0 and 14.6 cm^{-1}, respectively. Thus, the center frequency is lower and the bandwidth broadening is less significant in aprotic solvents compared with protic ones. Note that the spectra of its nitrile, isonitrile, and azido analogs in DMF (TFE) are centered at 2250.2, 2151.6, and 2103.6 (2268.9, 2180.7, and 2115.9) cm^{-1} with bandwidths of 11.0, 10.6, and 26.4 (19.8, 24.7, and 26.0) cm^{-1}, respectively.[30,31] Thus, the CN stretch frequencies in **1** are red-shifted from those in its nitrile analog but more blue-shifted from the NC and N_3 stretch frequencies in its isonitrile and azido analogs. The frequency blue shift of **1** in TFE relative to DMF is 20.2 cm^{-1}, whereas that of its nitrile, isonitrile, and azido analogs between the two solvents is 18.7, 29.1, and 12.3 cm^{-1}, respectively. Thus, the H-bond sensitivity of cyanamide is similar to that of nitrile but lower and higher than that of isonitrile and azide, respectively.

The CN stretch spectra of **2** in both polar protic and aprotic solvents exhibit characteristic complicated line shapes (see Figure 2b and Table S2 in the Supporting Information). Just in the case of D_2O, the spectrum of **2** could be fitted to a single Voigt peak centered at 2231.4 cm^{-1} with a bandwidth of 16.5 cm^{-1}. Note that a narrower bandwidth, possibly an indicator of the less inhomogeneous distribution of H-bond geometry around the NDCN group, was observed for **2** in comparison to **1**. In other three protic solvents, the spectra of **2** appear to be a doublet, which can be easily fitted to two Voigt peaks. The center frequencies of the low (high)-frequency peak are 2223.1, 2220.4, and 2227.4 (2247.5, 2243.1, and 2253.5) cm^{-1} and their bandwidths are 24.1, 26.2, and 27.7 (28.2, 23.9, and 33.2) cm^{-1} for H_2O, CH_3OH, and TFE, respectively. Thus, the more pronounced frequency blue shift (CH_3OH < H_2O < TFE for both low- and high-frequency peaks) and bandwidth broadening (H_2O < CH_3OH < TFE (CH_3OH < H_2O < TFE) for

DOI: 10.1021/acs.jpcb.8b00887
J. Phys. Chem. B 2018, 122, 4035−4044

Table 2. Stabilization Energies of the Delocalization Interaction between Donor and Acceptor NBOs in Model Molecules[a]

	donor NBO (i)	acceptor NBO (j)	$E(2)$ (kcal/mol)
CH_3NHCN	BD (1) C1−N2	BD*(2) C3−N4 (π_x*)	1.86
	BD (1) C1−N2	BD*(3) C3−N4 (π_y*)	3.40
	BD (1) N2−C3	BD*(2) C3−N4 (π_x*)	0.99
	BD (1) N2−H8	BD*(2) C3−N4 (π_x*)	1.86
	BD (1) N2−H8	BD*(3) C3−N4 (π_y*)	5.53
	BD (2) C3−N4	BD*(2) C3−N4 (π_x*)	0.51
	LP (1) N2	BD*(2) C3−N4 (π_x*)	27.94
C_6H_5NHCN	BD (1) C1−N7	BD*(3) C8−N9 (π_y*)	2.07
	BD (1) N7−H15	BD*(3) C8−N9 (π_y*)	5.23
	BD (2) C8−N9	BD*(2) C8−N9 (π_x*)	0.59
	LP (1) N7	BD*(2) C8−N9 (π_x*)	47.73
CH_3CN	BD (1) C1−H4	BD*(2) C2−N3 (π_y*)	6.90
	BD (1) C1−H5	BD*(2) C2−N3 (π_y*)	1.78
	BD (1) C1−H5	BD*(3) C2−N3 (π_x*)	5.12
	BD (1) C1−H6	BD*(2) C2−N3 (π_y*)	1.67
	BD (1) C1−H6	BD*(3) C2−N3 (π_x*)	5.23
C_6H_5CN	BD (1) C1−C2	BD*(2) C7−N8 (π_y*)	1.73
	BD (2) C1−C2	BD*(3) C7−N8 (π_x*)	17.60
	BD (1) C1−C6	BD*(2) C7−N8 (π_y*)	1.73
	BD* (2) C1−C2	BD*(3) C7−N8 (π_x*)	20.00

[a]The NBO label gives the type (BD for 2-center bond, LP for 1-center valence lone pair, and BD* for 2-center antibond), a serial number in parenthesis (1, 2, 3, ..., for the same type of bonds), the atom(s) to which the NBO is affixed (see Figure S6 in the Supporting Information for the numbering of atoms of four molecules). The z-axis is pointing toward the N atom of the C≡N bond. The x-axis is perpendicular to the phenyl ring in aromatics and to the plane containing the three atoms (H5-C1-N2 for CH_3NHCN and H4-C1-C2 for CH_3CN) in aliphatics. Note that the $E(2)$ values listed here are only for most of the CN π* acceptor orbitals.

low (high)-frequency peak) in proportion to the H-bond donating ability of the protic solvents (CH_3OH < H_2O < TFE) were also observed for **2** as is the case for **1**.[72] Note that the largest frequency blue shift and bandwidth broadening in TFE were also observed for **2** as is the case for **1**.[73,74] The solvatochromic behavior of **2** was observed to be also somewhat different from that of **1**. The broader bandwidth was observed for **2**, whereas the narrower bandwidth was observed for **1** in these three protic solvents compared with D_2O. In addition, when comparing the spectra of **2** in H_2O and CH_3OH, the smaller frequency blue shift was observed for both low- and high-frequency peaks in CH_3OH and the larger and smaller bandwidth broadenings were observed for low- and high-frequency peaks in CH_3OH, respectively. In the case of **1**, however, the slightly smaller frequency blue shift and slightly larger bandwidth broadening were observed in H_2O. In aprotic solvents, the spectra of **2** appear to be complicated with three Voigt peaks. The center frequencies of the low-, middle-, and high-frequency peaks are 2201.6, 2219.3, and 2235.1 (2201.8, 2215.1, and 2233.8) cm^{-1} and their bandwidths are 19.9, 16.9, and 18.4 (16.2, 15.7, and 23.5) cm^{-1} for DMF (DMSO), respectively. Thus, the lower center frequency and less significant bandwidth broadening in aprotic solvents compared with protic ones were also observed for **2** as is the case for **1**. Interestingly, the spectra of **2** in DMF and DMSO are similar despite the difference in solvent polarity between two solvents (dielectric constants of 36.7 and 46.7 for DMF and DMSO, respectively). Note that the spectra of its nitrile, isonitrile, and azido analogs in DMF (TFE) are centered at 2227.0, 2125.0, and 2118.9 (2243.8, 2159.0, and 2123.9) cm^{-1} with a bandwidth of 6.6, 7.6, and 22.7 (16.2, 22.7, and 26.6) cm^{-1}.[31] Thus, as is the case for **1**, the red-shifted and more blue-shifted CN stretch frequencies of cyanamide from the CN and NC (N_3) stretch frequencies of nitrile and isonitrile (azide), respectively, are also observed for **2** despite the notable line shape difference between **1** and **2** in DMF.

The CN stretch spectra of **2** obtained by deuteration with D_2O followed by dissolution in deuterated protic and aprotic solvents exhibit substantially simplified line shapes (see Figure 2c and Table S3 in the Supporting Information). In the cases of D_2O and CD_3OD, the spectra of **2** are a singlet centered at 2231.4 and 2231.7 cm^{-1} with bandwidths of 16.5 and 14.0 cm^{-1}, respectively. In the cases of DMF-d_7 and DMSO-d_6, the spectra of **2** are a doublet with low (high)-frequency peaks centered at 2224.3 and 2222.4 (2236.1 and 2237.6) cm^{-1} with bandwidths of 9.4 and 9.9 (15.5 and 11.4) cm^{-1}, respectively. Thus, two or three peaks are merged into a single peak with a narrower bandwidth upon deuteration of the NHCN into NDCN group. As will be discussed below, a complicated line shape of the CN stretch spectra in **2** having the NHCN instead of NDCN group arises from the Fermi resonance. A simple removal of the Fermi resonance by a deuterium substitution of just one exchangeable proton placed away from the main IR chromophore is unprecedented and can be an important design principle for novel IR probes.

To explain the complicated line shape of the CN stretch spectra in **2**, we carried out the peak assignment. Considering the spectra of **2** in H_2O, CH_3OH, and TFE, we assumed that the two peaks in these solvents originate from the two types of the NHCN group (H-bonded versus non-H-bonded to solvents). Then, we assumed that the spectra of **2** in their deuterated solvents are still a doublet but with red-shifted frequencies for the same two types of the NDCN group. However, this possibility is ruled out because the spectra of **2** in D_2O and CD_3OD were observed to be a singlet rather than a doublet. To obtain the information about the spectral behavior of **2** in protic solvents, we conducted harmonic and anharmonic frequency calculations using Gaussian 09 suite of packages for

DOI: 10.1021/acs.jpcb.8b00887
J. Phys. Chem. B 2018, 122, 4035−4044

four model systems (CH_3X and C_6H_5X in H_2O (X = NHCN) and D_2O (X = NDCN) with the Onsager continuum solvation model). The model systems used and the calculated frequencies are shown in Figure S5 and Table S4 in the Supporting Information, respectively. Harmonic frequency calculations for all model systems show that their CN stretch spectra are a singlet at ~2310−2320 cm^{-1}. Therefore, harmonic frequency calculations do not give us any clues about the possible source of the complicated line shape observed for **2** in protic solvents. However, anharmonic frequency calculations shed some light on this problem by providing the quantitative information about the overtones, combination modes, and the possible Fermi resonances among the vibrational modes. The calculation results reveal that there is one notable Fermi resonance between the CN stretch mode of the NHCN group and one of the overtones of the phenyl ring vibrations in C_6H_5NHCN (see the Fermi resonance between the harmonic frequency mode 15 (2310.8 cm^{-1}) and the overtone of the harmonic frequency mode 30 (1150.5 cm^{-1}) for C_6H_5NHCN in Table S4 in the Supporting Information). Note that this ring distortion mode also includes the N and H atoms from the NHCN group. Upon deuteration of the NHCN into NDCN group, the substantial frequency shifts of some of the phenyl ring vibrations at 1000−1700 cm^{-1} occur without any significant frequency shifts of the CN stretch mode. As a result, there is no possible Fermi resonance between the CN stretch mode of the NDCN group and the overtones (or combination modes) of the phenyl ring vibrations in C_6H_5NDCN. In the case of CH_3NHCN and CH_3NDCN, there is no phenyl ring in the structure anymore; thus, the possibility of the overtone (or combination mode) creation needed for its subsequent Fermi resonance with the NHCN and NDCN groups is eliminated.

As described earlier, the transition dipole strength of cyanamide is much larger than that of nitrile. In addition, the transition dipole strength of aliphatic cyanamide is comparable to that of aromatic cyanamide, whereas the much smaller transition dipole strength is observed for aliphatic nitrile in comparison to aromatic one. To explain such differences in transition dipole strengths between cyanamide and nitrile and between their aromatics and aliphatics, we performed the natural bond orbital (NBO) analyses for four model molecules (CH_3X and C_6H_5X (X = NHCN and CN)) using a Gaussian program (Figure S6 in the Supporting Information). The stabilization energy, $E(2)$, of the delocalization interaction between donor NBO (i) and acceptor NBO (j) is estimated as

$$E(2) = q_i \frac{F(i, j)^2}{E_j - E_i} \quad (2)$$

where q_i is the donor orbital occupancy, E_i and E_j are the donor and acceptor orbital energies, respectively, and $F(i, j)$ is the interaction (Fock matrix) element between donor and acceptor orbitals. The stabilization energies of the donor−acceptor NBO delocalization interaction are summarized in Table 2. The larger transition dipole strength of aromatic nitrile in comparison to aliphatic one can be understood by noting that the strong conjugation between the π bonding (π) and antibonding (π^*) orbitals of the phenyl ring and the antibonding (π^*) orbital of the CN group occurs only in C_6H_5CN but not in CH_3CN. The stabilization energy of the conjugation between the phenyl ring π (π^*) and CN π^* orbitals is ~17.6 (20.0) kcal/mol for C_6H_5CN. Such conjugation strengthens the C−C bond between the phenyl ring and CN group and weakens the C≡N bond. A similar phenomenon has been observed for the CO binding to heme, where π backbonding between Fe d_π and CO π^* orbitals results in the increase of the transition dipole strength of the CO stretch mode.[75] Likewise, the weakening of the C≡N bond upon conjugation of the phenyl ring π (π^*) and CN π^* orbitals leads to the much larger transition dipole strength and the nonnegligibly red-shifted frequency of aromatic nitrile relative to aliphatic one. In C_6H_5NHCN, the CN group is separated from the phenyl ring by an N atom and thus the π and π^* orbital conjugation taking place in C_6H_5CN no longer occurs. However, the lone pair electrons of the nitrogen are highly delocalized to the π^* orbital of the CN group in C_6H_5NHCN and even in CH_3NHCN. The stabilization energies of the conjugation between the nitrogen lone pair and CN π^* orbitals are ~27.9 and 47.7 kcal/mol for CH_3NHCN and C_6H_5NHCN, respectively. A similar kind of the delocalization pattern between the nitrogen lone pair and two CN p orbitals was discussed earlier for HNHCN but it was not connected to the transition dipole strength of cyanamide.[76] On the basis of the NBO analysis results, we propose the nitrogen lone pair delocalization onto the CN π^* orbital as an amplifier of IR absorption (Figure 3). Such delocalization interaction leads to

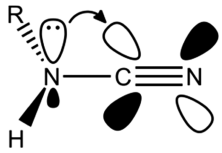

Figure 3. n → π^* interaction between the N atom's nonbonding orbital (n) and CN group's antibonding orbital (π^*) of the NHCN group.

the much larger transition dipole strength and the red-shifted frequency of cyanamide relative to nitrile and to the comparable transition dipole strength and the negligibly red-shifted frequency of aromatic cyanamide relative to the aliphatic one.

III.II. Polarization-Controlled IR Pump−Probe Spectroscopy. To determine the vibrational lifetimes of the CN stretch mode in cyanamide probes, the polarization-controlled IR pump−probe (IR PP) measurements for **1** and **2** were carried out using the experimental setup described earlier. A typical IR PP spectrum consists of positive and negative peaks in the high- and low-frequency regions, respectively. The positive peak arises from ground-state bleach (ν = 0 → 1 transition) and stimulated emission (ν = 1 → 0 transition), whereas the negative peak arises from excited-state absorption (ν = 1 → 2 transition).

First, we tried to obtain the IR PP spectra of **2** in water. However, the sample solubility in this solvent was too low to obtain the good-quality IR PP signal. In addition, all of the polar aprotic solvents including DMF were eliminated because of the too complicated spectral line shape, which mostly make the data analysis impossible. Afterward, we managed to measure the IR PP spectra of **2** in methanol but the results were still far from satisfactory because of its weak signal. Finally, a mixture of CH_3OD and DMSO in a volume ratio of 1:1 was used as a solvent in the IR PP measurement for **2**. DMSO in this solvent mixture acted to lower the background from CH_3OD and to increase the sample solubility, which finally led to the high-

DOI: 10.1021/acs.jpcb.8b00887
J. Phys. Chem. B 2018, 122, 4035−4044

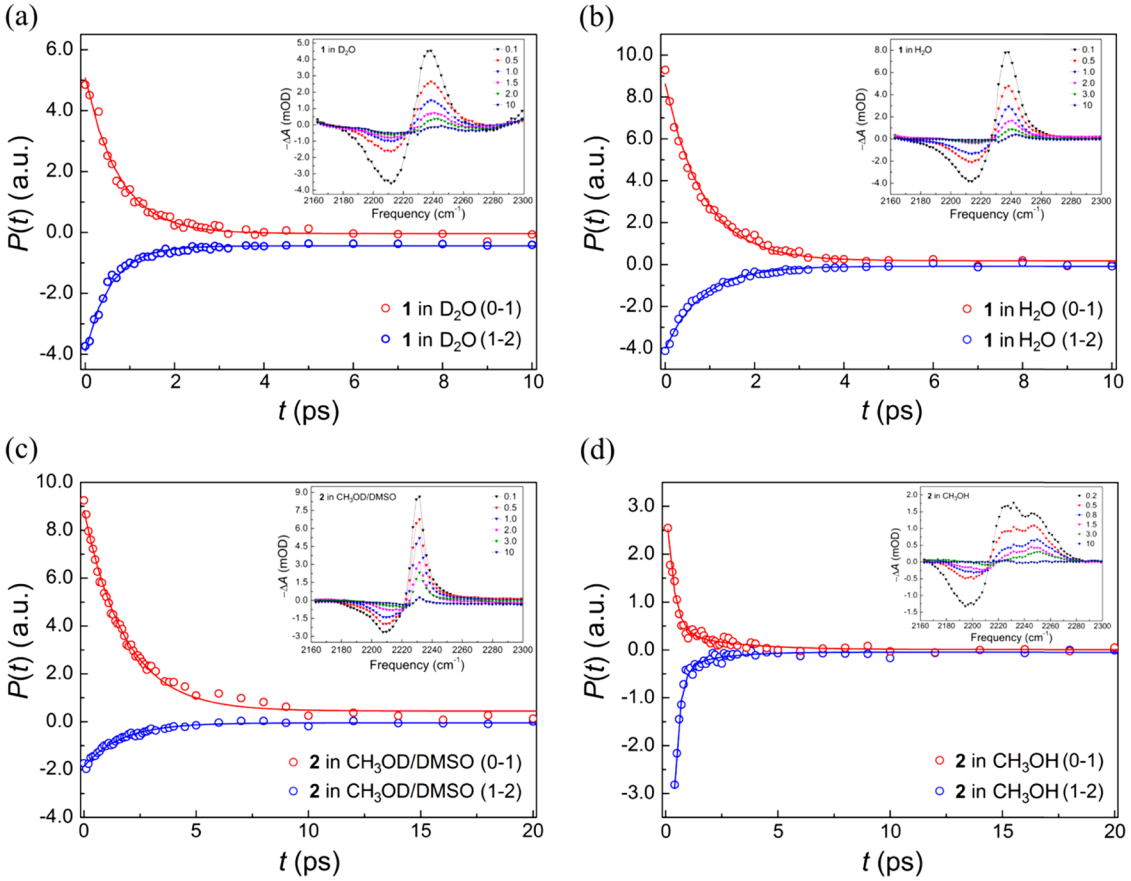

Figure 4. Vibrational population decays of **1** in D_2O (a) and H_2O (b) and **2** in CH_3OD/DMSO (1:1 v/v) mixture (c) and CH_3OH (d). In (a) and (c), the samples were deuterated by their direct dissolution in D_2O and CH_3OD/DMSO, respectively. The inset shows the isotropic transient absorption spectra at delay time t (ps). These plots were obtained from the IR pump−probe data shown in Figure S7 in the Supporting Information. The time-dependent intensities of the transient absorption at two selected probe frequencies (2212 and 2236 cm^{-1} in **1** and 2203 and 2232 cm^{-1} in **2**) for the 1−2 and 0−1 transitions in (a)−(c) were fitted to a single-exponential decay function, whereas those in (d) were fitted to a double-exponential decay function. The fitting parameters are shown in Table S5 in the Supporting Information.

quality IR PP signal unobtainable for **2** in CH_3OD alone. In contrast, CH_3OD in this solvent mixture acted to prevent the formation of a complicated spectral line shape observed for **2** in DMSO alone. The FTIR spectrum of **2** in DMSO is well fitted to three peaks but changed to a single peak upon the addition of CH_3OD. The added CH_3OD deuterates the NHCN into NDCN group and thus prevents the Fermi resonance responsible for a complicated spectral line shape.

The IR PP data analyses for **1** in D_2O and H_2O and **2** in CH_3OD/DMSO (1:1 v/v) mixture and CH_3OH are presented in Figure 4 and Table 1. The time profile of the peak intensities of the isotropic transient absorption spectra at a selected frequency was fitted to a single-exponential decay function for **1** in D_2O and H_2O and **2** in CH_3OD/DMSO, whereas it was fitted to a double-exponential decay function for **2** in CH_3OH. Subsequently, the vibrational lifetimes obtained using the aforementioned method at different frequencies (∼2195−2220 cm^{-1} for the negative peak and ∼2230−2250 cm^{-1} for the positive peak) were averaged. The vibrational lifetimes of the CN stretch mode in **1** were determined to be 0.58 ± 0.04 ps in D_2O and 0.89 ± 0.09 ps in H_2O and those in **2** to be 1.64 ± 0.13 ps in CH_3OD/DMSO and 0.30 ± 0.05 and 2.62 ± 0.26 ps in CH_3OH. Note that two time components were observed only for **2** in CH_3OH, where the amplitude of the short time component is quite large (78%), indicating that the majority of the vibrational relaxation occurs within the first 300 fs. In addition, as mentioned above, the Fermi resonance occurs from the strong coupling between the CN stretch and phenyl ring vibrations, opening an ultrafast relaxation channel of CN excitation to low-frequency phenyl ring vibrations.[31,57] Thus, the short time component observed for **2** in CH_3OH is attributed to the vibrational relaxation through Fermi resonance. Note that the vibrational lifetimes of the isonitrile and azido groups in their alanine analogs are 5.5 and 1.1 ps in D_2O and 5.5 and 1.3 ps in DMF and those of the nitrile, isonitrile, and azido groups in their phenylalanine analogs are 4.8, 10.5, and 8.4 ps in DMF, respectively.[30,31] Thus, the vibrational lifetimes of the cyanamide group are close to those of the nitrile and azido groups but shorter than those of the isonitrile group.

IV. SUMMARY

In this work, we studied the vibrational properties of terminally blocked cyanamide (NHCN)-derivatized alanine **1** and phenylalanine **2** using FTIR and ultrafast IR pump−probe methods in combination with quantum chemical calculations. First of all, the transition dipole strength of cyanamide is found to be much larger than that of nitrile but comparable to that of isonitrile and azide. Thus, the larger transition dipole strength was observed for CN bonded to N atom in comparison to C, S, and Se atoms.[30,31,41] The vibrational frequency of cyanamide is red-shifted from that of nitrile but more blue-shifted from that of

DOI: 10.1021/acs.jpcb.8b00887
J. Phys. Chem. B 2018, 122, 4035−4044

isonitrile and azide. Thus, the smaller frequency red shift from CN bonded to C atom was observed for CN bonded to N atom in comparison to S and Se atoms.[30,31,41] A similar frequency red shift from CN bonded to C atom between CN bonded to S and Se atoms and NC bonded to C atom was observed.[30,31,41] The vibrational lifetime of cyanamide is close to that of nitrile and azide but shorter than that of isonitrile. Thus, the far smaller thermal insulation effect enhancing the vibrational dynamic range was observed for CN bonded to C and N atoms in comparison to S and Se atoms.[30,31,41] Taken together, CN bonded to N atom is similar to CN bonded to C in vibrational frequency and lifetime but to NC bonded to C atom in transition dipole strength. We believe that CN bonded to N atom can be a strongly absorbing IR reporter of the conformational and environmental structure and dynamics of biomolecules in comparison to CN bonded to C, a weak absorber.

To explain the much larger transition dipole strength and the red-shifted frequency of cyanamide relative to nitrile, quantum chemical calculations were performed. We found that such differences are associated with the presence and absence of the $n \rightarrow \pi^*$ interaction between the N atom's nonbonding (n) and CN group's antibonding (π^*) orbitals in cyanamide and nitrile, respectively. Note that the larger transition dipole strength and the red-shifted frequency of isonitrile relative to nitrile are possibly associated with the stronger (weaker) donor−acceptor interaction between the NC (CN) group's neighboring (σ, π, or π^*) and antibonding (π^*) orbitals in isonitrile (nitrile).[30] Quantum chemical calculations also reveal that a complicated line shape of the CN stretch spectra in aromatic cyanamide is attributed to the Fermi resonance between the CN stretch mode of the NHCN group and one of the overtones of the phenyl ring vibrations, which does not occur in aromatic nitrile.

■ ASSOCIATED CONTENT

Supporting Information

The Supporting Information is available free of charge on the ACS Publications website at DOI: 10.1021/acs.jpcb.8b00887.

Complete author list for ref 71; detailed synthetic procedures and characterization; figures and tables showing the additional results of spectroscopic and computational studies (PDF)

■ AUTHOR INFORMATION

Corresponding Authors

*E-mail: hogyuhan@korea.ac.kr (H.H.).
*E-mail: kkwak@korea.ac.kr (K.K.).
*E-mail: mcho@korea.ac.kr (M.C.).

ORCID

Dorota Kossowska: 0000-0002-5758-6642
Minhaeng Cho: 0000-0003-1618-1056

Author Contributions

‖G.L. and D.K. contributed equally to this work.

Notes

The authors declare no competing financial interest.

■ ACKNOWLEDGMENTS

This work was supported by IBS-R023-D1. H.H. is grateful for the financial support from the National Research Foundation (NRF) of Korea funded by the Ministry of Science, ICT, and Future Planning (NRF2016R1A2B4013572).

■ REFERENCES

(1) Cho, M. *Two-Dimensional Optical Spectroscopy*; CRC Press: Boca Raton, FL, 2009.
(2) Hamm, P.; Zanni, M. *Concepts and Methods of 2D Infrared Spectroscopy*; Cambridge University Press: New York, NY, 2011.
(3) Ganim, Z.; Chung, H. S.; Smith, A. W.; DeFlores, L. P.; Jones, K. C.; Tokmakoff, A. Amide I Two-Dimensional Infrared Spectroscopy of Proteins. *Acc. Chem. Res.* **2008**, *41*, 432−441.
(4) Cho, M. Coherent Two-Dimensional Optical Spectroscopy. *Chem. Rev.* **2008**, *108*, 1331−1418.
(5) Le Sueur, A. L.; Horness, R. E.; Thielges, M. C. Applications of Two-Dimensional Infrared spectroscopy. *Analyst* **2015**, *140*, 4336−4349.
(6) Ghosh, A.; Ostrander, J. S.; Zanni, M. T. Watching Proteins Wiggle: Mapping Structures with Two-Dimensional Infrared Spectroscopy. *Chem. Rev.* **2017**, *117*, 10726−10759.
(7) Waegele, M. M.; Culik, R. M.; Gai, F. Site-Specific Spectroscopic Reporters of the Local Electric Field, Hydration, Structure, and Dynamics of Biomolecules. *J. Phys. Chem. Lett.* **2011**, *2*, 2598−2609.
(8) Kim, H.; Cho, M. Infrared Probes for Studying the Structure and Dynamics of Biomolecules. *Chem. Rev.* **2013**, *113*, 5817−5847.
(9) Ma, J.; Pazos, I. M.; Zhang, W.; Culik, R. M.; Gai, F. Site-Specific Infrared Probes of Proteins. *Annu. Rev. Phys. Chem.* **2015**, *66*, 357−377.
(10) Gosavi, P. M.; Korendovych, I. V. Minimalist IR and Fluorescence Probes of Protein Function. *Curr. Opin. Chem. Biol.* **2016**, *34*, 103−109.
(11) Adhikary, R.; Zimmermann, J.; Romesberg, F. E. Transparent Window Vibrational Probes for the Characterization of Proteins With High Structural and Temporal Resolution. *Chem. Rev.* **2017**, *117*, 1927−1969.
(12) Błasiak, B.; Londergan, C. H.; Webb, L. J.; Cho, M. Vibrational Probes: From Small Molecule Solvatochromism Theory and Experiments to Applications in Complex Systems. *Acc. Chem. Res.* **2017**, *50*, 968−976.
(13) Andrews, S. S.; Boxer, S. G. Vibrational Stark Effects of Nitriles I. Methods and Experimental Results. *J. Phys. Chem. A* **2000**, *104*, 11853−11863.
(14) Andrews, S. S.; Boxer, S. G. Vibrational Stark Effects of Nitriles II. Physical Origins of Stark Effects from Experiment and Perturbation Models. *J. Phys. Chem. A* **2002**, *106*, 469−477.
(15) Suydam, I. T.; Boxer, S. G. Vibrational Stark Effects Calibrate the Sensitivity of Vibrational Probes for Electric Fields in Proteins. *Biochemistry* **2003**, *42*, 12050−12055.
(16) Fang, C.; Bauman, J. D.; Das, K.; Remorino, A.; Arnold, E.; Hochstrasser, R. M. Two-Dimensional Infrared Spectra Reveal Relaxation of the Nonnucleoside Inhibitor TMC278 Complexed with HIV-1 Reverse Transcriptase. *Proc. Natl. Acad. Sci. U.S.A.* **2008**, *105*, 1472−1477.
(17) Weeks, C. L.; Polishchuk, A.; Getahun, Z.; DeGrado, W. F.; Spiro, T. G. Investigation of an Unnatural Amino Acid for Use as a Resonance Raman Probe: Detection Limits and Solvent and Temperature Dependence of the νC≡N Band of 4-Cyanophenylalanine. *J. Raman Spectrosc.* **2008**, *39*, 1606−1613.
(18) Bian, H.; Zhao, W.; Zheng, J. Intermolecular Vibrational Energy Exchange Directly Probed with Ultrafast Two Dimensional Infrared Spectroscopy. *J. Chem. Phys.* **2009**, *131*, No. 124501.
(19) Taskent-Sezgin, H.; Chung, J.; Patsalo, V.; Miyake-Stoner, S. J.; Miller, A. M.; Brewer, S. H.; Mehl, R. A.; Green, D. F.; Raleigh, D. P.; Carrico, I. Interpretation of *p*-Cyanophenylalanine Fluorescence in Proteins in Terms of Solvent Exposure and Contribution of Side-Chain Quenchers: A Combined Fluorescence, IR and Molecular Dynamics Study. *Biochemistry* **2009**, *48*, 9040−9046.
(20) Lindquist, B. A.; Furse, K. E.; Corcelli, S. A. Nitrile Groups as Vibrational Probes of Biomolecular Structure and Dynamics: An Overview. *Phys. Chem. Chem. Phys.* **2009**, *11*, 8119−8132.
(21) Zimmermann, J.; Thielges, M. C.; Seo, Y. J.; Dawson, P. E.; Romesberg, F. E. Cyano Groups as Probes of Protein Microenvironments and Dynamics. *Angew. Chem., Int. Ed.* **2011**, *50*, 8333−8337.

DOI: 10.1021/acs.jpcb.8b00887
J. Phys. Chem. B 2018, 122, 4035−4044

(22) Bagchi, S.; Fried, S. D.; Boxer, S. G. A Solvatochromic Model Calibrates Nitriles' Vibrational Frequencies to Electrostatic Fields. *J. Am. Chem. Soc.* **2012**, *134*, 10373−10376.
(23) Chung, J. K.; Thielges, M. C.; Fayer, M. D. Conformational Dynamics and Stability of HP35 Studied with 2D IR Vibrational Echoes. *J. Am. Chem. Soc.* **2012**, *134*, 12118−12124.
(24) Levinson, N. M.; Fried, S. D.; Boxer, S. G. Solvent-Induced Infrared Frequency Shifts in Aromatic Nitriles Are Quantitatively Described by the Vibrational Stark Effect. *J. Phys. Chem. B* **2012**, *116*, 10470−10476.
(25) Rodgers, J. M.; Zhang, W.; Bazewicz, C. G.; Chen, J.; Brewer, S. H.; Gai, F. Kinetic Isotope Effect Provides Insight into the Vibrational Relaxation Mechanism of Aromatic Molecules: Application to Cyano-Phenylalnine. *J. Phys. Chem. Lett.* **2016**, *7*, 1281−1287.
(26) Basom, E. J.; Maj, M.; Cho, M.; Thielges, M. C. Site-Specific Characterization of Cytochrome P450cam Conformations by Infrared Spectroscopy. *Anal. Chem.* **2016**, *88*, 6598−6606.
(27) Silverman, L. N.; Pitzer, M. E.; Ankomah, P. O.; Boxer, S. G.; Fenlon, E. E. Vibrational Stark Effect Probes for Nucleic Acids. *J. Phys. Chem. B* **2007**, *111*, 11611−11613.
(28) Krummel, A. T.; Zanni, M. T. Evidence for Coupling between Nitrile Groups Using DNA Templates: A Promising New Method for Monitoring Structures with Infrared Spectroscopy. *J. Phys. Chem. B* **2008**, *112*, 1336−1338.
(29) Gillies, A. T.; Gai, X. S.; Buckwalter, B. L.; Fenlon, E. E.; Brewer, S. H. ^{15}N NMR Studies of a Nitrile-Modified Nucleoside. *J. Phys. Chem. B* **2010**, *114*, 17136−17141.
(30) Maj, M.; Ahn, C.; Kossowska, D.; Park, K.; Kwak, K.; Han, H.; Cho, M. β-Isocyanoalanine as an IR Probe: Comparison of Vibrational Dynamics between Isonitrile and Nitrile-Derivatized IR Probes. *Phys. Chem. Chem. Phys.* **2015**, *17*, 11770−11778.
(31) Maj, M.; Ahn, C.; Błasiak, B.; Kwak, K.; Han, H.; Cho, M. Isonitrile as an Ultrasensitive Infrared Reporter of Hydrogen-Bonding Structure and Dynamics. *J. Phys. Chem. B* **2016**, *120*, 10167−10180.
(32) Fafarman, A. T.; Webb, L. J.; Chuang, J. I.; Boxer, S. G. Site-Specific Conversion of Cysteine Thiols into Thiocyanate Creates an IR Probe for Electric Fields in Proteins. *J. Am. Chem. Soc.* **2006**, *128*, 13356−13357.
(33) Maienschein-Cline, M. G.; Londergan, C. H. The CN Stretching Band of Aliphatic Thiocyanate is Sensitive to Solvent Dynamics and Specific Solvation. *J. Phys. Chem. A* **2007**, *111*, 10020−10025.
(34) Fafarman, A. T.; Sigala, P. A.; Herschlag, D.; Boxer, S. G. Decomposition of Vibrational Shifts of Nitriles into Electrostatic and Hydrogen-Bonding Effects. *J. Am. Chem. Soc.* **2010**, *132*, 12811−12813.
(35) Sokolowsky, K. P.; Fayer, M. D. Dynamics in the Isotropic Phase of Nematogens Using 2D IR Vibrational Echo Measurements on Natural-Abundance ^{13}CN and Extended Lifetime Probes. *J. Phys. Chem. B* **2013**, *117*, 15060−15071.
(36) Johnson, M. N. R.; Londergan, C. H.; Charkoudian, L. K. Probing the Phosphopantetheine Arm Conformations of Acyl Carrier Proteins Using Vibrational Spectroscopy. *J. Am. Chem. Soc.* **2014**, *136*, 11240−11243.
(37) Levin, D. E.; Schmitz, A. J.; Hines, S. M.; Hines, K. J.; Tucker, M. J.; Brewer, S. H.; Fenlon, E. E. Synthesis and Evaluation of the Sensitivity and Vibrational Lifetimes of Thiocyanate and Selenocyanate Infrared Reporters. *RSC Adv.* **2016**, *6*, 36231−36237.
(38) Ramos, S.; Scott, K. J.; Horness, R. E.; Le Sueur, A. L.; Thielges, M. C. Extended Timescale 2D IR Probes of Proteins: *p*-Cyanoselenophenylalanine. *Phys. Chem. Chem. Phys.* **2017**, *19*, 10081−10086.
(39) Zheng, J.; Kwak, K.; Xie, J.; Fayer, M. D. Ultrafast Carbon-Carbon Single-Bond Rotational Isomerization in Room-Temperature Solution. *Science* **2006**, *313*, 1951−1955.
(40) Xuan, W.; Li, J.; Luo, X.; Schultz, P. G. Genetic Incorporation of a Reactive Isothiocyanate Group into Proteins. *Angew. Chem., Int. Ed.* **2016**, *55*, 10065−10068.
(41) Park, K.-H.; Jeon, J.; Park, Y.; Lee, S.; Kwon, H.-J.; Joo, C.; Park, S.; Han, H.; Cho, M. Infrared Probes Based on Nitrile-Derivatized Prolines: Thermal Insulation Effect and Enhanced Dynamic Range. *J. Phys. Chem. Lett.* **2013**, *4*, 2105−2110.
(42) Maj, M.; Oh, Y.; Park, K.; Lee, J.; Kwak, K.-W.; Cho, M. Vibrational Dynamics of Thiocyanate and Selenocyanate Bound to Horse Heart Myoglobin. *J. Chem. Phys.* **2014**, *140*, No. 235104.
(43) Maj, M.; Kwak, K.; Cho, M. Ultrafast Structural Fluctuations of Myoglobin-Bound Thiocyanate and Selenocyanate Ions Measured with Two-Dimensional Infrared Photon Echo Spectroscopy. *ChemPhysChem* **2015**, *16*, 3468−3476.
(44) Błasiak, B.; Ritchie, A. W.; Webb, L. J.; Cho, M. Vibrational Solvatochromism of Nitrile Infrared Probes: Beyond the Vibrational Stark Dipole Approach. *Phys. Chem. Chem. Phys.* **2016**, *18*, 18094−18111.
(45) Oh, K.-I.; Lee, J.-H.; Joo, C.; Han, H.; Cho, M. β-Azidoalanine as an IR Probe: Application to Amyloid Aβ(16−22) Aggregation. *J. Phys. Chem. B* **2008**, *112*, 10352−10357.
(46) Oh, K.-I.; Kim, W.; Joo, C.; Yoo, D.-G.; Han, H.; Hwang, G.-S.; Cho, M. Azido Gauche Effect on the Backbone Conformation of β-Azidoalanine Peptides. *J. Phys. Chem. B* **2010**, *114*, 13021−13029.
(47) Lee, K.-K.; Park, K.-H.; Joo, C.; Kwon, H.-J.; Han, H.; Ha, J.; Park, S.; Cho, M. Ultrafast Internal Rotational Dynamics of the Azido Group in (4*S*)-Azidoproline: Chemical Exchange 2DIR Spectroscopic Investigations. *Chem. Phys.* **2012**, *396*, 23−29.
(48) Lee, K.-K.; Park, K.-H.; Joo, C.; Kwon, H.-J.; Jeon, J.; Jung, H.-I.; Park, S.; Han, H.; Cho, M. Infrared Probing of 4-Azidoproline Conformations Modulated by Azido Configurations. *J. Phys. Chem. B* **2012**, *116*, 5097−5110.
(49) Choi, J.-H.; Raleigh, D.; Cho, M. Azido Homoalanine is a Useful Infrared Probe for Monitoring Local Electrostatistics and Side-Chain Solvation in Proteins. *J. Phys. Chem. Lett.* **2011**, *2*, 2158−2162.
(50) Thielges, M. C.; Axup, J. Y.; Wong, D.; Lee, H. S.; Chung, J. K.; Schultz, P. G.; Fayer, M. D. Two-Dimensional IR Spectroscopy of Protein Dynamics Using Two Vibrational Labels: A Site-Specific Genetically Encoded Unnatural Amino Acid and an Active Site Ligand. *J. Phys. Chem. B* **2011**, *115*, 11294−11304.
(51) Tookmanian, E. M.; Fenlon, E. E.; Brewer, S. H. Synthesis and Protein Incorporation of Azido-Modified Unnatural Amino Acids. *RSC Adv.* **2015**, *5*, 1274−1281.
(52) Tookmanian, E. M.; Phillips-Piro, C. M.; Fenlon, E. E.; Brewer, S. H. Azidoethoxyphenylalanine as a Vibrational Reporter and Click Chemistry Partner in Proteins. *Chem. - Eur. J.* **2015**, *21*, 19096−19103.
(53) Gai, X. S.; Fenlon, E. E.; Brewer, S. H. A Sensitive Multispectroscopic Probe for Nucleic Acids. *J. Phys. Chem. B* **2010**, *114*, 7958−7966.
(54) Tucker, M. J.; Gai, X. S.; Fenlon, E. E.; Brewer, S. H.; Hochstrasser, R. M. 2D IR Photon Echo of Azido-Probes for Biomolecular Dynamics. *Phys. Chem. Chem. Phys.* **2011**, *13*, 2237−2241.
(55) Gai, X. S.; Coutifaris, B. A.; Brewer, S. H.; Fenlon, E. E. A Direct Comparison of Azide and Nitrile Vibrational Probes. *Phys. Chem. Chem. Phys.* **2011**, *13*, 5926−5930.
(56) Schmitz, A. J.; Hogle, D. G.; Gai, X. S.; Fenlon, E. E.; Brewer, S. H.; Tucker, M. J. Two-Dimensional Infrared Study of Vibrational Coupling between Azide and Nitrile Reporters in a RNA Nucleoside. *J. Phys. Chem. B* **2016**, *120*, 9387−9394.
(57) Nydegger, M. W.; Dutta, S.; Cheatum, C. M. Two-Dimensional Infrared Study of 3-Azidopyridine as a Potential Spectroscopic Reporter of Protonation State. *J. Chem. Phys.* **2010**, *133*, No. 134506.
(58) Lipkin, J. S.; Song, R.; Fenlon, E. E.; Brewer, S. H. Modulating Accidental Fermi Resonance: What a Difference a Neutron Makes. *J. Phys. Chem. Lett.* **2011**, *2*, 1672−1676.
(59) Wolfshorndl, M. P.; Baskin, R.; Dhawan, I.; Londergan, C. H. Covalently Bound Azido Groups Are Very Specific Water Sensors, Even in Hydrogen-Bonding Environments. *J. Phys. Chem. B* **2012**, *116*, 1172−1179.
(60) Tucker, M. J.; Kim, Y. S.; Hochstrasser, R. M. 2D IR Photon Echo Study of the Anharmonic Coupling in the OCN Region of Phenyl Cyanate. *Chem. Phys. Lett.* **2009**, *470*, 80−84.

DOI: 10.1021/acs.jpcb.8b00887
J. Phys. Chem. B 2018, 122, 4035−4044

(61) Lee, K.-K.; Park, K.-H.; Choi, J.-H.; Ha, J.-H.; Jeon, S.-J.; Cho, M. Ultrafast Vibrational Spectroscopy of Cyanophenols. *J. Phys. Chem. A* **2010**, *114*, 2757−2767.
(62) Remorino, A.; Korendovych, I. V.; Wu, Y.; DeGrado, W. F.; Hochstrasser, R. M. Residue-Specific Vibrational Echoes Yield 3D Structures of a Transmembrane Helix Dimer. *Science* **2011**, *332*, 1206−1209.
(63) Kratochvil, H. T.; Carr, J. K.; Matulef, K.; Annen, A. W.; Li, H.; Maj, M.; Ostmeyer, J.; Serrano, A. L.; Raghuraman, H.; Moran, S. D.; et al. Instantaneous Ion Configurations in the K^+ Ion Channel Selectivity Filter Revealed by 2D IR Spectroscopy. *Science* **2016**, *353*, 1040−1044.
(64) Kratochvil, H. T.; Maj, M.; Matulef, K.; Annen, A. W.; Ostmeyer, J.; Perozo, E.; Roux, B.; Valiyaveetil, F. I.; Zanni, M. T. Probing the Effects of Gating on the Ion Occupancy of the K^+ Channel Selectivity Filter Using Two-Dimensional Infrared Spectroscopy. *J. Am. Chem. Soc.* **2017**, *139*, 8837−8845.
(65) Woys, A. M.; Mukherjee, S. S.; Skoff, D. R.; Moran, S. D.; Zanni, M. T. A Strongly Absorbing Class of Non-Natural Labels for Probing Protein Electrostatics and Solvation with FTIR and 2D IR Spectroscopies. *J. Phys. Chem. B* **2013**, *117*, 5009−5018.
(66) Peran, I.; Oudenhoven, T.; Woys, A. M.; Watson, M. D.; Zhang, T. O.; Carrico, I.; Zanni, M. T.; Raleigh, D. P. General Strategy for the Bioorthogonal Incorporation of Strongly Absorbing, Solvation-Sensitive Infrared Probes into Proteins. *J. Phys. Chem. B* **2014**, *118*, 7946−7953.
(67) Lam, Z.; Kong, K. V.; Olivo, M.; Leong, W. K. Vibrational Spectroscopy of Metal Carbonyls for Bio-Imaging and -Sensing. *Analyst* **2016**, *141*, 1569−1586.
(68) Moilanen, D. E.; Piletic, I. R.; Fayer, M. D. Water Dynamics in Nafion Fuel Cell Membranes: The Effects of Confinement and Structural Changes on the Hydrogen Bond Network. *J. Phys. Chem. C* **2007**, *111*, 8884−8891.
(69) Becke, A. D. Density-Functional Exchange-Energy Approximation with Correct Asymptotic Behavior. *Phys. Rev. A* **1988**, *38*, 3098−3100.
(70) Lee, C.; Yang, W.; Parr, R. G. Development of the Colle-Salvetti Correlation-Energy Formula into a Functional of the Electron Density. *Phys. Rev. B* **1988**, *37*, 785−789.
(71) Frisch, M. J.; Trucks, G. W.; Schlegel, H. B.; Scuseria, G. E.; Robb, M. A.; Cheeseman, J. R.; Scalmani, G.; Barone, V.; Mennucci, B.; Petersson, G. A.; et al. *Gaussian 09*, revision E.01; Gaussian, Inc.: Wallingford, CT, 2009.
(72) Kamlet, M. J.; Abboud, J.-L. M.; Abraham, M. H.; Taft, R. W. Linear Solvation Energy Relationships. 23. A Comprehensive Collection of the Solvatochromic Parameters, π^*, α, and β, and Some Methods for Simplifying the Generalized Solvatochromic Equation. *J. Org. Chem.* **1983**, *48*, 2877−2887.
(73) Heger, M.; Scharge, T.; Suhm, M. A. From Hydrogen Bond Donor to Acceptor: The Effect of Ethanol Fluorination on the First Solvating Water Molecule. *Phys. Chem. Chem. Phys.* **2013**, *15*, 16065−16073.
(74) Hansen, A. S.; Du, L.; Kjaergaard, H. G. The Effect of Fluorine Substitution in Alcohol-Amine Complexes. *Phys. Chem. Chem. Phys.* **2014**, *16*, 22882−22891.
(75) Hill, J. R.; Dlott, D. D.; Rella, C. W.; Peterson, K. A.; Decatur, S. M.; Boxer, S. G.; Fayer, M. D. Vibrational Dynamics of Carbon Monoxide at the Active Sites of Mutant Heme Proteins. *J. Phys. Chem.* **1996**, *100*, 12100−12107.
(76) Davies, M.; Jones, W. J. The Infra-red Spectrum and Structure of Cyanamide and Dimethylcyanamide. *Trans. Faraday Soc.* **1958**, *54*, 1454−1463.
(77) Qu, X.; Lee, E.; Yu, G.-S.; Freedman, T. B.; Nafie, L. A. Quantitative Comparison of Experimental Infrared and Raman Optical Activity Spectra. *Appl. Spectrosc.* **1996**, *50*, 649−657.

DOI: 10.1021/acs.jpcb.8b00887
J. Phys. Chem. B 2018, 122, 4035−4044